

## PLATELETS AND THROMBOPOIESIS

## Platelet transactivation by monocytes promotes thrombosis in heparin-induced thrombocytopenia

Valerie Tutwiler,<sup>1,2</sup> Daria Madeeva,<sup>2</sup> Hyun Sook Ahn,<sup>2</sup> Izabella Andrianova,<sup>3</sup> Vincent Hayes,<sup>2</sup> X. Long Zheng,<sup>4</sup> Douglas B. Cines,<sup>5</sup> Steven E. McKenzie,<sup>6</sup> Mortimer Poncz,<sup>2,7</sup> and Lubica Rauova<sup>2,7</sup>

<sup>1</sup>School of Biomedical Engineering, Science, and Health Systems, Drexel University, Philadelphia, PA; <sup>2</sup>Department of Pediatrics, Children's Hospital of Philadelphia, Philadelphia PA; <sup>3</sup>Institute of Fundamental Medicine and Biology, Kazan Federal University, Kazan, Russia; <sup>4</sup>Division of Laboratory Medicine, Department of Pathology, University of Alabama at Birmingham, Birmingham, AL; <sup>5</sup>Department of Pathology and Laboratory Medicine, Perelman School of Medicine, University of Pennsylvania, Philadelphia, PA; <sup>6</sup>Department of Medicine, Thomas Jefferson University, Philadelphia, PA; and <sup>7</sup>Department of Pediatrics, Perelman School of Medicine, University of Pennsylvania, Philadelphia, PA

## Key Points

- The procoagulant nature of HIT can be simulated in a microfluidic model using human blood and its components.
- PF4/glycosaminoglycans/immunoglobulin G complexes activate monocytes through Fc $\gamma$ RIIA to generate TF and thrombin, leading to coated platelets in HIT.

**Heparin-induced thrombocytopenia (HIT) is characterized by a high incidence of thrombosis, unlike other antibody-mediated causes of thrombocytopenia. We have shown that monocytes complexed with surface-bound platelet factor 4 (PF4) activated by HIT antibodies contribute to the prothrombotic state in vivo, but the mechanism by which this occurs and the relationship to the requirement for platelet activation via fragment crystallizable (Fc) $\gamma$ RIIA is uncertain. Using a microfluidic model and human or murine blood, we confirmed that activation of monocytes contributes to the prothrombotic state in HIT and showed that HIT antibodies bind to monocyte Fc $\gamma$ RIIA, which activates spleen tyrosine kinase and leads to the generation of tissue factor (TF) and thrombin. The combination of direct platelet activation by HIT immune complexes through Fc $\gamma$ RIIA and transactivation by monocyte-derived thrombin markedly increases Annexin V and factor Xa binding to platelets, consistent with the formation of procoagulant coated platelets. These data provide a model of HIT wherein a combination of direct Fc $\gamma$ RIIA-mediated platelet activation and monocyte-derived thrombin contributes to thrombosis in HIT and identifies potential new targets for lessening this risk. (*Blood*. 2016;127(4):464-472)**

## Introduction

Heparin-induced thrombocytopenia (HIT) is an iatrogenic, immune-mediated disorder characterized by antibodies that recognize complexes between the platelet chemokine platelet factor 4 (PF4, CXCL4) and heparin or cell surface glycosaminoglycans (GAGs).<sup>1,2</sup> It is estimated that up to 50% of patients with HIT develop thrombosis that might be limb- and/or life-threatening.<sup>3-5</sup> Even with early recognition, cessation of heparin, and institution of alternative forms of anticoagulation, recurrent thromboembolic complications may occur and 10% to 20% of patients go on to amputation and/or death.<sup>6</sup> Thus, there is a need for a better understanding of the pathogenesis of HIT and to determine how this information can be used to mitigate the risk of thrombosis.

Thrombocytopenia and thrombosis in HIT have been attributed to binding of PF4/heparin/immunoglobulin G (IgG) immune-complexes to the platelets through the IgG fragment crystallizable (Fc) region, which activates platelets through their immunoreceptor tyrosine-based activation motif (ITAM) receptor, Fc $\gamma$ RIIA.<sup>7,8</sup> However, monocytes, endothelial cells, and other cell types might also be activated by these immune complexes and contribute to the underlying pathology,<sup>9</sup> but their contribution to the process is less well characterized. Indeed, recent evidence suggests that thrombosis in HIT is initiated by binding

of pathogenic antibodies to antigenic complexes of PF4 and GAGs expressed by the endothelium as well as circulating cells, including monocytes.<sup>10,11</sup> Although platelets are an important target for activating HIT antibodies, their GAGs primarily consist of chondroitin sulfate, which has a lower affinity for PF4<sup>12,13</sup> than the more complex mixture of GAGs expressed on monocytes.<sup>14,15</sup> In line with this finding, we have shown that HIT antibodies bind with greater avidity to monocytes than to platelets in the presence of PF4, and this binding is more resistant to dissociation by high concentrations of heparin.<sup>11</sup> This leaves the question open as to why platelet activation leads to thrombosis in HIT<sup>16</sup> rather than bleeding, as seen in most other settings of immune thrombocytopenia.

In a passive immunization murine model of HIT generated by a murine HIT-like monoclonal antibody (mAb) KKO,<sup>10</sup> we showed that monocyte depletion by clodronate-laden liposome infusions decreased carotid artery thrombosis induced by photochemical injury, while paradoxically exacerbating thrombocytopenia.<sup>11</sup> However, the multiplicity of potential pathways operative in this in vivo setting did not afford us the opportunity to dissect the sequence of cellular interactions leading to thrombosis and whether activation of monocytes amplifies platelet sensitivity to HIT immune complexes. Using a microfluidic

Submitted November 27, 2013; accepted October 21, 2015. Prepublished online as *Blood* First Edition paper, October 30, 2015; DOI 10.1182/blood-2013-11-539262.

The online version of this article contains a data supplement.

The publication costs of this article were defrayed in part by page charge payment. Therefore, and solely to indicate this fact, this article is hereby marked "advertisement" in accordance with 18 USC section 1734.

© 2016 by The American Society of Hematology

system, we now extend these findings to a wholly human system to define the steps involved in monocyte activation. We show that monocytes activated through their Fc $\gamma$ RIIA provide a second signal, which augments immune complex-mediated platelet activation and contributes to the intensely prothrombotic nature of HIT. The clinical implications of these findings are discussed.

## Material and methods

### Recombinant proteins

Wild-type (WT) human PF4 (hPF4) in plasmid pMT/BiP/V5-His (Invitrogen) was expressed using the Drosophila Expression System (Invitrogen), purified, and characterized as described.<sup>2</sup> Total protein concentrations were determined using the bicinchoninic acid protein assay (Pierce) with bovine serum albumin (BSA) as the standard.

Human von Willebrand factor (VWF) was purified from outdated plasma by precipitation and gel filtration as described previously.<sup>17</sup> The plasmid encoding full-length mouse VWF (mVWF) was a kind gift from Dr David Motto (Pudget Sound Blood Center). Recombinant mVWF was purified from Dulbecco's modified Eagle medium/Ham F-12 medium serum-free conditioned medium of HEK293 cells stably transfected with Lipofectamine 2000 using Q-fast flow ion exchange column, followed by Sephacryl S-300 (GE Healthcare) gel filtration. The purity of the final product was determined by 10% sodium dodecyl sulfate-polyacrylamide gel electrophoresis with Coomassie Blue staining. Quantification was performed using the absorbance 280 nm and 1 cm cuvette (1 optical density = 1 mg/mL). The size distribution of purified mVWF was determined by 1% agarose gel electrophoresis.

### Antibodies

KKO and the nonpathogenic anti-hPF4-specific mAb RTO are both mouse IgG (mIgG) 2b.<sup>18</sup> Polyclonal HIT human IgGs (hIgG) were isolated using a recombinant protein G-agarose column (Invitrogen) as described by us,<sup>10</sup> from the plasma of patients with the clinically presumptive diagnosis of HIT<sup>19</sup> and who were also positive by the HIT enzyme-linked immunosorbent assay and serotonin release assay.<sup>20</sup> Control IgGs were isolated from the plasmas of healthy subjects. HIT IgG reactivity with PF4/heparin complexes was confirmed by enzyme-linked immunosorbent assay.<sup>18</sup> Anti-factor X (FX) mAb 4G3 (a kind gift from Dr Rodney Camire, Children's Hospital of Philadelphia [CHOP]), and Fab fragments from a rat anti-mouse CD41 antibody (BD Pharmingen) were labeled using the Alexa Fluor 405 and Alexa Fluor 488 Protein Labeling Kits (Molecular Probes), respectively. Phycoerythrin (PE) labeled anti-human P-selectin and anti-human (h)CD32, and PerCP-Cy5.5-labeled anti-hCD41 mAbs were from BD Biosciences and fluorescein isothiocyanate-labeled Annexin V was from Abcam. Blocking anti-mouse tissue factor (TF) mAb 1H1<sup>21</sup> was a kind gift of Dr Daniel Kirchhofer (Genentech). The blocking antibody against Fc $\gamma$ RIIA (IV.3) was derived from the IV.3 hybridoma cell line (American Type Culture Collection), and Fab fragments were prepared using a Fab Preparation Kit (Thermo Scientific). Blocking mouse anti-human antibodies against Fc $\gamma$ RI (CD64, clone 10.1) and Fc $\gamma$ RIII (CD16, clone 3G8) were from BD Pharmingen and BioLegend, respectively. mIgG1 (clone MG1-45; BioLegend) was used as the isotype control blocking antibody and mIgG2b (clone eBMG2b; eBioscience) was the KKO isotype control.

### Murine and human blood samples

Transgenic mice expressing platelet hPF4 and/or Fc $\gamma$ RIIA (hPF4<sup>+</sup>, Fc $\gamma$ RIIA<sup>+</sup>, and hPF4<sup>+</sup>/Fc $\gamma$ RIIA<sup>+</sup> mice) were described previously.<sup>11</sup> All mice were also *pf4* gene-deleted, termed PF4<sup>null</sup> mouse.<sup>22</sup> Mouse blood was drawn from the inferior vena cava using a protocol approved by the Institutional Animal Care and Use Committee at CHOP into a syringe containing sodium citrate (final concentration, 12.9 mM) and immediately diluted 1:1 (v/v) in modified Tyrode's buffer (134 mM NaCl, 3 mM KCl, 0.3 mM NaH<sub>2</sub>PO<sub>4</sub>, 2 mM MgCl<sub>2</sub>, 5 mM N-2-hydroxyethylpiperazine-N'-2-ethanesulfonic acid [HEPES], 5 mM glucose,

12 mM NaHCO<sub>3</sub>, and 0.1% BSA; Sigma A7030) containing PGE1 (final concentration, 1  $\mu$ g/mL; Sigma).

Human blood was collected after informed consent from healthy, aspirin-free volunteers using a 19-gauge butterfly needle in 129 mM sodium citrate (10:1, v/v) under a protocol approved by CHOP's Institutional Review Board for studies involving human subjects. Thrombin-inhibited blood was obtained by drawing human blood into D-phenylalanyl-L-propyl-L-arginine chloromethyl ketone (PPACK) (final concentration, 100  $\mu$ M; Calbiochem).

### Isolated blood cells

Monocytes were depleted from whole human blood using Dynabeads CD14 (Invitrogen). Depletion was >95% efficient as assessed by flow cytometry using a combination of anti-CD45/CD14 mAbs (see supplemental Figure 1, available on the *Blood* Web site) in whole blood. Human monocytes for repletion experiments were isolated from whole blood by negative selection using the Monocyte Isolation Kit II (Miltenyi Biotec) per the manufacturer's instructions. Isolated monocytes were incubated with appropriate blocking anti-Fc $\gamma$ Rs or control antibodies (50  $\mu$ g/mL), or with a selective inhibitor of the spleen tyrosine kinase (Syk) PRT318<sup>23</sup> (kindly provided by Dr Uma Sinha, Portola Pharmaceuticals; final concentration, 3  $\mu$ M) or with its solvent, dimethyl-sulfoxide for 30 minutes. After washing with phosphate-buffered saline (PBS) with 0.1% BSA, 2.5  $\times$  10<sup>5</sup>, monocytes were added back to monocyte-depleted blood (final volume, 500  $\mu$ L). Mouse monocytes were isolated from transgenic Fc $\gamma$ RIIA<sup>+</sup>/mouse PF4 (mPF4)<sup>null</sup> and mPF4<sup>null</sup> mice by negative selection using EasySep Mouse Monocyte Isolation Kit (Stemcell Technologies). Mouse platelet-rich plasma (PRP) was isolated from diluted Fc $\gamma$ RIIA<sup>+</sup>/mPF4<sup>null</sup> blood after centrifugation for 5 minutes at 180 g and mixed with isolated monocytes in the ratio of 1 to 1.5 monocytes per 1000 platelets. The final contamination of platelets from the monocyte sample was <1%.

### Flow cytometry

Unmodified, monocyte-depleted, and monocyte-repleted whole blood or PRP samples were incubated in Ca<sup>++</sup>/HEPES buffer (2.5 mM CaCl<sub>2</sub>, 1.25 mM MgCl<sub>2</sub>, 150 mM NaCl, 10 mM HEPES, pH 7.5) 1/100 (v/v) in the presence of 10 mM of Gly-Pro-Arg-Pro-NH<sub>2</sub> peptide (Bachem H-1998), PerCP-Cy 5.5 labeled anti-hCD41, PE-labeled anti-P-selectin, and Alexa 405-labeled anti-FX antibodies with either PF4 (10  $\mu$ g/mL) plus KKO (50  $\mu$ g/mL) or PF4 (10  $\mu$ g/mL) plus RTO (50  $\mu$ g/mL) for 45 minutes at 37°C. To optimize the incubation time for stimulation by PF4 + KKO, control samples stimulated with thrombin plus convulxin<sup>24</sup> were included, and the incubation times with PF4 plus KKO were varied. At the end of the incubation, samples were transferred to ice, diluted with 4 volumes of Ca<sup>++</sup>/HEPES buffer with Annexin V fluorescein isothiocyanate (Abcam), and analyzed by flow cytometry (LSRFortessa, BD Biosciences). Platelets were gated based on the forward-scatter and CD41 fluorescence parameters, and binding of Annexin V, anti-FX, and anti-P-selectin antibodies was quantified as geometric mean fluorescent intensity (MFI).

### Analysis of microfluidic thrombosis

A well-plate microfluidic device (Fluxion Biosciences, San Francisco, CA) was used to analyze platelet adhesion and aggregation (hereafter referred to as platelet accretion) and thrombus formation.<sup>25</sup> Microfluidic channels were coated for 1 hour at room temperature with a 25  $\mu$ L volume of PBS containing 20  $\mu$ g/mL of mVWF or hVWF, washed with PBS, and then blocked with 0.5% BSA in PBS. Whole blood samples were incubated for 30 minutes at 37°C with hPF4 (10  $\mu$ g/mL) and either a specific mAb (KKO, RTO, or isotype control) at 50  $\mu$ g/mL or polyclonal hIgG at 1.0 mg/mL. The concentration of hPF4 chosen was at the low end of the levels of PF4 that we have shown can trigger HIT,<sup>10</sup> as we anticipated that additional platelet activation would increase the available PF4.<sup>26</sup> Blood samples were added to the inlet well, after which the chambers were perfused at a shear rate of 20 dyne/cm<sup>2</sup> (500 s<sup>-1</sup>) at 37°C. Control experiments in which the incubation time with PF4 plus KKO and shear rate were varied to optimize conditions. Final conditions described for the assay are those that maximized platelet accretion. In initial studies performed to establish the model, only platelet accretion was followed. To label human platelets, 3  $\mu$ M calcein AM (Invitrogen) was added to whole

blood; mouse platelets were labeled with Alexa 488 conjugated anti-mouse CD41 Fab fragment (final concentration, 1.2  $\mu\text{g}/\text{mL}$ ). Human and mouse samples were perfused for 3 or 5 minutes, respectively, images were acquired every 3 to 10 seconds, and the data were analyzed with BioFlux Montage software (Fluxion Biosciences) using the automated modules for percent covered area at each time point and aggregate size at the end point. Image and video acquisition was performed using an Eclipse TE2000-U inverted microscope (Nikon, Japan) employing a CoolSNAP ES camera (Photometrics) and NIS-Elements Acquisition software (version 3.20). After upgrading the acquisition system, multicolor image and video acquisition in Fc $\gamma$ R blocking experiments was performed using an Axio Observer Z1 microscope (Zeiss, Germany) employing a Fluxion CCD camera (10.9 fps, 1392  $\times$  1040 pixels, 6.45  $\mu\text{m}$  pixel size; QImaging, Canada) and BioFlux Montage control and acquisition software (Fluxion Biosciences). Samples were re-calcified to 5 mM CaCl<sub>2</sub> immediately prior to the perfusion and fibrin deposition was visualized by adding Alexa 561- or Alexa 647-labeled fibrinogen (Invitrogen) to the whole blood (1.5  $\mu\text{g}/\text{mL}$ ). Images were acquired every 60 seconds for 15 minutes. Fibrin deposition was first detected 6 to 8 minutes after the onset of perfusion. At the end of the experiment, channels were washed with PBS/EDTA, fixed with 2% paraformaldehyde (BD Biosciences), and studied by confocal microscopy using an Axio Observer inverted microscope (Zeiss LSM710) and Zeiss ZEN 2011 software. Images were analyzed using Volocity version 6.1 (PerkinElmer) to determine the total fluorescence intensity of the labeled fibrinogen volume in 3 dimensions.

### Statistical analysis

The experimental data were analyzed for statistical differences using Prism 5.0 software (GraphPad). Two-tailed Student *t* tests (paired when appropriate) with an  $\alpha$  value of 0.05 were used when comparing the platelet accretion or fibrin deposition between two samples. An analysis of variance (repeated measures when appropriate) was used to compare platelet accretion or fibrin deposition data between 3 or more groups. The analysis of variance was followed by a Tukey post hoc analysis to determine statistically significant differences. A Wilcoxon Signed-Rank test was used to compare ratios to a hypothetical value of 1, which corresponds to no effect, to assess the consistency of changes in outcome. The Wilcoxon Signed-Rank test was followed by a one-sample *t* test to determine the significance of the fold change.

## Results

### In vitro model of platelet accretion and fibrin deposition

We established a microfluidic system to investigate the mechanism by which monocytes are activated in HIT and its relationship to platelet activation seen in the passive immunization model of this disorder. Experiments were performed under controlled shear conditions equivalent to blood flow in small arteries<sup>27</sup> using species-specific VWF-coated surfaces. Initial studies were performed to determine if this ex vivo system recapitulated the prothrombotic state seen in the passive immunization model of HIT. Whole blood from hPF4<sup>+</sup> and/or Fc $\gamma$ RIIA<sup>+</sup> transgenic mice were each incubated with KKO to induce a HIT-like state, and then perfused over a surface coated with mVWF. As in the murine HIT model,<sup>10,28</sup> blood from double-transgenic hPF4<sup>+</sup>/Fc $\gamma$ RIIA<sup>+</sup> mice caused a 6  $\pm$  threefold (mean  $\pm$  standard error of the mean [SEM]) increase in platelet accretion (adhesion plus aggregation) within the channel field ( $P < .01$ ) (Figure 1A), and a 19  $\pm$  ninefold increase in average aggregate size ( $P < .001$ ) (Figure 1B) when stimulated with the HIT-like mAb KKO compared with stimulation with the nonpathogenic anti-PF4 mAb RTO. In contrast, KKO and RTO produced identical results when added to blood from single transgenic hPF4<sup>+</sup> or Fc $\gamma$ RIIA<sup>+</sup> mice (Figure 1A-B). These results closely recapitulate findings in the cremaster arteriole laser injury model<sup>11</sup> (supplemental Figure 2).

We then established a similar, but “humanized” microfluidic system by adding hPF4 (10  $\mu\text{g}/\text{mL}$ ) followed by KKO (50  $\mu\text{g}/\text{mL}$ ) to whole blood samples from normal volunteers.<sup>10</sup> Similar to findings in blood from the double-transgenic mice, KKO caused a 1.7  $\pm$  0.2-fold increase in total platelet accretion compared with RTO ( $P < .01$ ) (Figure 1C) and a 15.1  $\pm$  14.6-fold increase in aggregate size ( $P < .01$ ) (Figure 1D). Moreover, 4 of 5 preparations of IgG from patients with HIT (1 mg/mL) gave similar outcomes when compared with normal IgG (Figure 1E). Because only ~1% to 2% of the total patient IgG is antigen-specific,<sup>29</sup> it was expected that 20-fold high concentrations would be necessary to produce outcomes comparable to KKO. These studies demonstrate that the perfusion system using human blood cells recapitulates the salient features of platelet activation seen in the murine model of HIT.

The addition of hPF4 followed by the addition of KKO to human whole blood also generated an extensive fibrin network radiating from the platelet aggregates typically aligned along the direction of flow (Figure 1F, right). In contrast, control samples exposed to hPF4 plus RTO showed little fibrin deposition and less organization (Figure 1F, left). KKO increased fibrin deposition 3.4  $\pm$  0.5-fold compared with either RTO or an isoimmune control IgG plus hPF4 ( $P < .05$ ).

### Involvement of monocytes in procoagulant processes

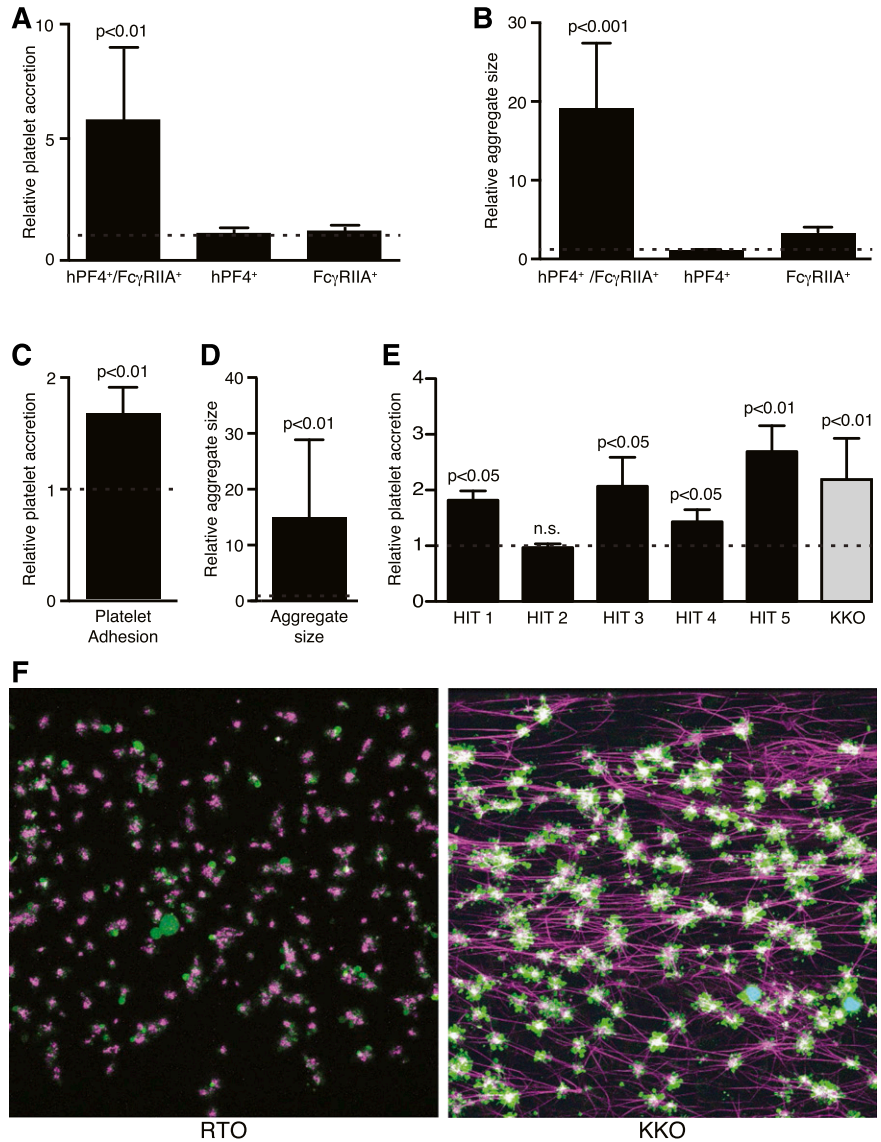
We next examined how and whether human monocytes contribute to platelet accretion and fibrin deposition in the microfluidic system. We began by depleting monocytes from samples of whole blood. Depletion of monocytes decreased platelet accretion by 70  $\pm$  9% ( $P < .01$ , compared with whole blood exposed to control beads without CD14 antibodies) (Figure 2A), and decreased fibrin deposition by 56  $\pm$  12% ( $P < .05$ , compared with control whole blood) (Figure 2B). Repletion of monocytes to the physiologic level of 5  $\times$  10<sup>5</sup> cells/mL restored the ability of KKO to stimulate platelet accretion and fibrin deposition to levels that did not differ significantly from that of unmodified, whole blood (Figure 2).

Previous in vitro<sup>7,8</sup> and in vivo<sup>30</sup> studies showed that signaling through Fc $\gamma$ RIIA on platelets is required for their activation by HIT antibodies and by KKO. On monocytes, however, Fc $\gamma$ RI has been implicated in the KKO-mediated generation of TF and monocyte microparticle formation.<sup>31</sup> Both Fc $\gamma$ RI and Fc $\gamma$ RIIA activation involves ITAM, which is rapidly phosphorylated upon receptor engagement followed by binding of Syk.<sup>32</sup> We previously reported that inhibition of the Syk pathway in platelets using the specific inhibitor PRT318 blocked the development of thrombocytopenia and thrombosis in the murine model of HIT.<sup>23</sup> Similarly, the addition of PRT318 to whole blood in vitro inhibited platelet accretion by 48  $\pm$  13% ( $P < .05$ ) at 3 minutes of perfusion and inhibited fibrin deposition by 82  $\pm$  4% ( $P < .05$ ) compared with vehicle control (Figure 3A). However, PRT318 inhibits Syk in all circulating cells. To study the importance of the Syk pathway in monocytes specifically, isolated monocytes were pre-incubated with PRT318 and then recombined with monocyte-depleted blood before adding hPF4 and KKO. Similar to results seen after monocyte depletion, selective inhibition of Syk in monocytes caused significant suppression of platelet accretion at 3 minutes of perfusion by 44  $\pm$  6% ( $P < .05$ ) and inhibition of fibrin deposition by 38  $\pm$  7% ( $P < .05$ ) (Figure 3B). This monocyte-specific inhibition by PRT318 points toward an important contribution of a Syk-based pathway in monocytes to the development of a prothrombotic state in HIT.

### Role of monocyte Fc $\gamma$ RI, RII, and RIII

We next evaluated the contribution of each of the 3 major classes of Fc $\gamma$ Rs expressed by human monocytes. To do so, blocking monoclonal

**Figure 1. In vitro microfluidic thrombosis model of HIT.** (A) Kinetic quantitative fluorescence analysis of platelet accretion to VWF-coated surfaces after perfusion of citrated whole blood from transgenic mice. Data are expressed as relative platelet accretion calculated from area under the curve (AUC) of percent area covered by platelets (AUC of sample stimulated with KKO divided by AUC of sample stimulated with RTO). Dotted line represents no additional activation with KKO compared with RTO. Mean  $\pm$  SEM is shown. N = 8, 6, and 5 for each transgenic line, respectively. (B) Same studies analyzed for relative platelet aggregate size. (C) Kinetic quantitative fluorescence analysis of platelet accretion to VWF-coated surfaces after perfusion of citrated whole human blood. Data are expressed as in (A). N = 7 with each experiment performed in duplicate. (D) Same as (B), using human blood. N = 7 with each experiment performed in duplicate. (E) Similar studies as in (C) conducted with isolated IgG from patients with clinically and serologically documented HIT compared with normal hlgG. Each HIT-IgG was tested with blood from 3 healthy donors, each done in 3 independent experiments. Dotted line represents no activation with the HIT IgG compared with normal control IgG. Two-tailed Student *t* tests were used to compare KKO-induced accretion and aggregate size vs the paired RTO control. (F) Representative confocal microscopy images of fixed thrombi formed in microfluidic channels. Platelet aggregates are shown in green, fibrin fibers visualized by adding of Alexa 647-labeled fibrinogen are purple, and white blood cells are cyan (overlap of blue nuclear dye is Hoechst and green calcein AM). The attachment points of fibrin to platelets are white because of superposition of purple and green colors. Images were acquired using a Zeiss LSM 710 AxioObserver inverted microscope (Germany) with a 40 $\times$  1.1 NA water immersion objective. n.s., not statistically significant following KKO vs RTO exposure.



IgGs directed against FcγRI (CD64, clone 10.1),<sup>33</sup> FcγRIIA (CD32; clone IV.3),<sup>34</sup> and FcγRIII (CD16; clone 3G8)<sup>35</sup> were added to whole blood or to isolated monocytes, which were then used to reconstitute

whole blood. In whole blood, blocking of FcγRIIA suppressed platelet accretion induced by KKO plus hPF4 by 52  $\pm$  5% (*P* < .0001) and decreased fibrin deposition by 62  $\pm$  5% (*P* < .0001) (Figure 4A-B,

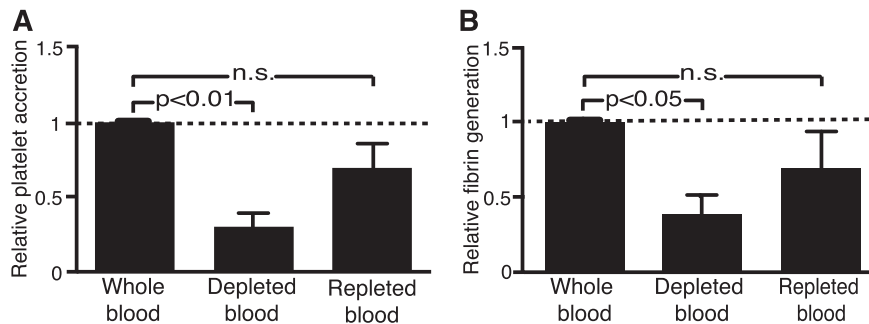


**Figure 2. Inhibition of KKO-induced platelet accretion and fibrin generation by monocyte depletion and partial restoration by monocyte repletion.** (A) Analysis of platelet accretion in the microfluidic system using human whole blood samples, blood samples after monocyte depletion, and samples repleted with monocytes isolated from a separate donor. All samples were run in parallel, stimulated with PF4 and KKO, and expressed relative to a whole blood control. Data are presented as the ratio of experimental to control conditions. Dotted line represents no stimulation or inhibition relative to whole blood sample. Mean  $\pm$  1 SEM is shown. N = 5 with samples from 3 donors. Paired Student *t* tests were used to compare depleted or repleted blood to the whole blood control. (B) Same as in (A), but for end point analysis of fibrin generation. n.s., not statistically significant comparing whole and repleted blood studies.

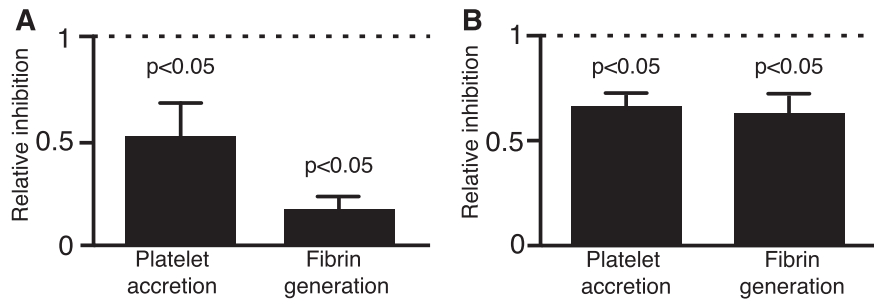


**Figure 3. Inhibition of KKO-induced platelet accretion and fibrin generation by PRT318.** (A) Inhibition of Syk signaling by PRT318 in whole human blood for platelet accretion and fibrin generation compared with vehicle control. Relative inhibition is shown as a ratio of sample pre-incubated with the Syk-pathway inhibitor and the sample incubated with the vehicle control. KKO plus PF4 was added to each and samples were run in parallel. Mean  $\pm$  1 SEM is shown. N = 3 with each experiment performed in triplicate. Paired two-tailed Student *t* tests were used to evaluate the significance of differences between samples with PRT318 and those with vehicle control. (B) Same as in (A), but using monocyte-targeted Syk inhibition prior to repleting monocyte-depleted blood.

respectively) as compared with the isotype control. Blocking Fc $\gamma$ RI or Fc $\gamma$ RIII did not affect platelet accretion or fibrin deposition relative to isotype controls (Figure 4A-B, respectively). Blocking of Fc $\gamma$ RIIA specifically in monocytes caused significant inhibition of fibrin deposition ( $52 \pm 8\%$ ,  $P < .005$ ) (Figure 4D), whereas comparable inhibition of Fc $\gamma$ RI or Fc $\gamma$ RIII did not. Platelet accumulation was also decreased by blocking Fc $\gamma$ RIIA, but did not reach statistical significance relative to isotype control (Figure 4C). Again, the blocking of Fc $\gamma$ RI or Fc $\gamma$ RIII on isolated monocytes prior to repletion did not significantly inhibit either platelet accretion or fibrin deposition (Figure 4C-D, respectively). To exclude the possibility that blocking mAbs leached from the monocytes and consequently directly blocked platelet Fc $\gamma$ RIIA-mediated activation in reconstituted blood, we examined the binding of PE-labeled anti-Fc $\gamma$ RIIA mAb, which is blocked by IV.3. Although binding of PE-labeled anti-Fc $\gamma$ RIIA mAb to platelets was completely blocked after incubation of whole blood with IV.3 Fab, there was only a minimal decrease in binding to platelets after targeted inhibition of monocyte Fc $\gamma$ RIIA (supplemental Figure 3).

### Effect of monocyte activation

Activation of monocytes might promote thrombosis in HIT by inducing the expression and release of TF,<sup>11,36</sup> leading to the generation of thrombin. To assess this possibility, blood taken from hPF4<sup>+</sup>/Fc $\gamma$ RIIA<sup>+</sup> and both single transgenic mice was incubated with the function blocking anti-mouse TF mAb 1H1 followed by the addition of KKO. Anti-TF antibody attenuated platelet accretion in whole blood from hPF4<sup>+</sup>/Fc $\gamma$ RIIA<sup>+</sup> mice by  $29 \pm 6\%$  ( $P < .02$  compared with isotype control), but had no effect on accretion of platelets from single transgenic hPF4<sup>+</sup> mice (Figure 5A). Additionally, inhibition of thrombin's proteolytic activity by PPACK<sup>37</sup> inhibited platelet accretion by  $29 \pm 7\%$  upon addition of KKO to whole blood ( $P < .0001$ ), but not following the addition of RTO (Figure 5B).

### Dual activation generates coated platelets

These studies suggest that thrombin generated on the surface of stimulated monocytes might activate platelets via protease-activated receptor 1 (PAR-1), augmenting the signal induced by engaging of

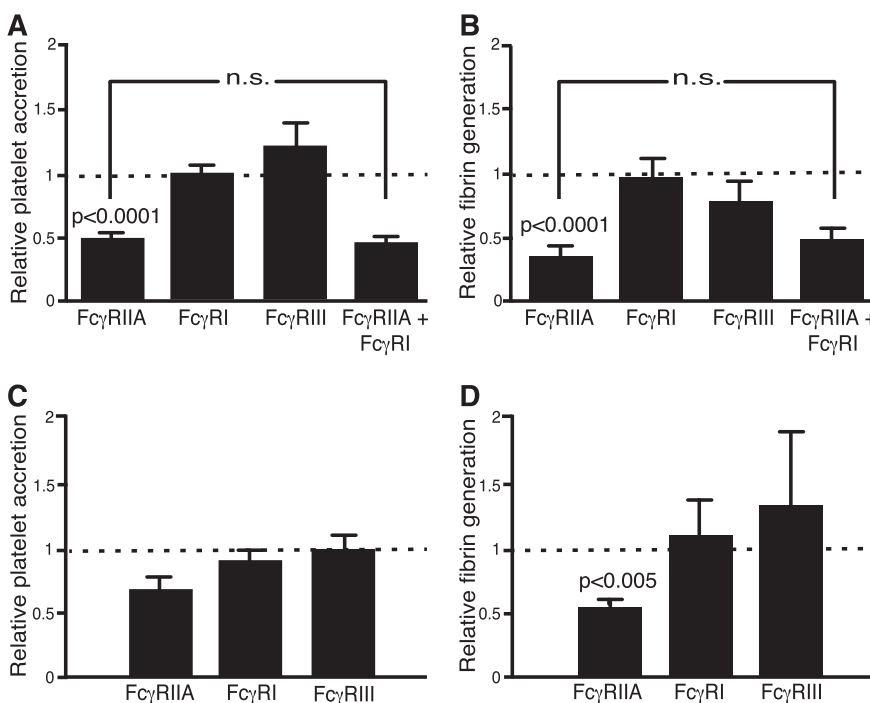


**Figure 4. Effect of Fc $\gamma$ R signaling pathways on KKO-induced platelet and fibrin accretion.** Fc $\gamma$ RIIA, Fc $\gamma$ RI, Fc $\gamma$ RIII, and Fc $\gamma$ RIIA plus Fc $\gamma$ RI signaling was blocked in whole blood samples as in studies shown in Figure 2 for (A) platelet accretion, and (B) fibrin generation. Relative platelet accretion and fibrin generation are expressed as the ratio of results from samples blocked with specific mAb to samples pre-incubated with isotype control. Mean  $\pm$  1 SEM is shown. Dotted line represents the relative value for the isotype control; values below the dotted line means inhibition after blockade of the indicated Fc $\gamma$ R compared with isotype control with *P* values shown relative to that control. Significance was determined using two-tailed Student *t* tests when comparing Fc $\gamma$ R to the isotype control, each stimulated with PF4 and KKO. N = 10 with samples from 5 donors. (C-D) are as (A-B) respectively, but with isolated monocytes that were then used to reconstitute whole blood as in Figure 3. n.s., not statistically significant between blocking Fc $\gamma$ RIIA and blocking Fc $\gamma$ RIIA plus Fc $\gamma$ RI.



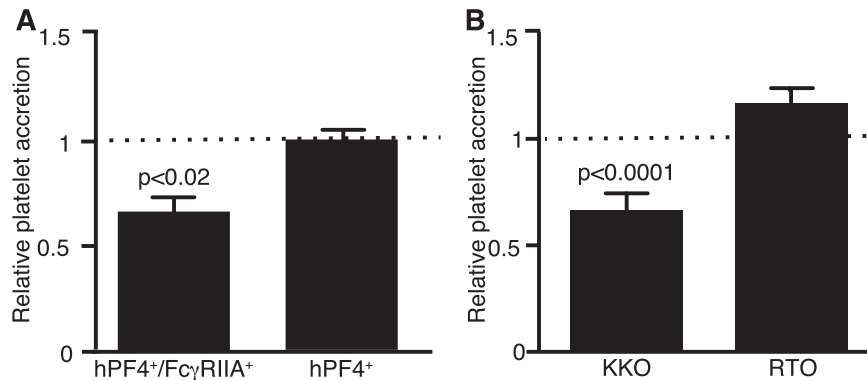


**Figure 5. Inhibition of the KKO-induced platelet accretion.** (A) Microfluidic study of platelet accretion performed as in Figure 1 using blood from the double transgenic hPF4<sup>+</sup>/FcγRIIA<sup>+</sup> mice and control hPF4<sup>+</sup> mice after blocking TF activity induced by KKO with 1H1 antibody. Mean ± 1 SEM is shown. Relative platelet accumulation is expressed as the ratio calculated from AUC of percent area covered by platelets (AUC of sample inhibited by 1H1/AUC of sample incubated with isotype control). Dotted line represents no inhibition of stimulation by KKO. 1H1 inhibited and isotype control samples were run in parallel, and the significance of the difference was determined using paired two-tailed Student *t* tests. N = 6 for double transgenic mice and N = 3 for the single transgenic mice. (B) Effect of PPACK inhibition of thrombin activity on platelet accretion in human whole blood was measured following activation with KKO or the anti-PF4 antibody RTO that does not activate platelets. All samples were run in parallel and data are expressed as in (A), as the ratio of PPACK-treated to vehicle control sample. N = 3 with each experiment performed in duplicate.

platelet FcγRIIA.<sup>38</sup> Coactivation of platelets via a G-protein–coupled receptor (GPCR), as PARs, and an ITAM pathway, as FcγRIIA, has been shown to lead to the formation of highly prothrombotic, coated platelets.<sup>39,40</sup> We therefore asked whether platelets stimulated with KKO and PF4 show changes in expression of surface markers consistent with formation of coated platelets.<sup>24</sup> Expression of P-selectin and binding of Annexin V and anti-FX antibodies to platelets, markers of coated platelets, all increased significantly following exposure of human blood to KKO and PF4 (Figure 6A). Expression of these activation markers was markedly diminished in the absence of monocytes either in PRP or in monocyte-depleted whole blood (Figure 6B). Blocking of FcγRIIA decreased platelet activation and formation of coated platelets, as in the microfluidic experiments (Figure 6C). Blocking of FcγRI, together with FcγRIIA, imparted no greater inhibition (Figure 6C). When monocytes were added back to monocyte-depleted blood following blockage of individual Fc receptor subtypes, an intact FcγRIIA, but not FcγRI or FcγRIII, was required to form coated platelets (Figure 6D).

To investigate further if FcγRIIA-dependent signaling in monocytes augments the effect on KKO and PF4 in platelets, we activated human or mouse FcγRIIA<sup>+</sup> platelets in the presence of FcγRIIA<sup>+</sup> or WT mouse monocytes that naturally lack FcγRIIA. Human platelets formed significantly more coated platelets in the presence of FcγRIIA<sup>+</sup> monocytes than in the presence FcγRIIA-deficient monocytes or in the absence of monocytes (PRP only), as characterized by binding of Annexin V and expression of surface-bound FXa, although there was no difference in the expression of P-selectin (Figure 6E). Similar results were obtained when isolated mouse monocytes were added to mouse FcγRIIA<sup>+</sup> platelets. In the presence of FcγRIIA<sup>+</sup> mouse monocytes, mouse platelets bound more Annexin V than in the presence of WT monocytes, but again there was no difference in P-selectin expression (supplemental Figure 4). These data further implicate monocytes, and specifically monocyte FcγRIIA, in the induction of coated platelets in HIT.

#### Inhibition of thrombin receptor PAR1

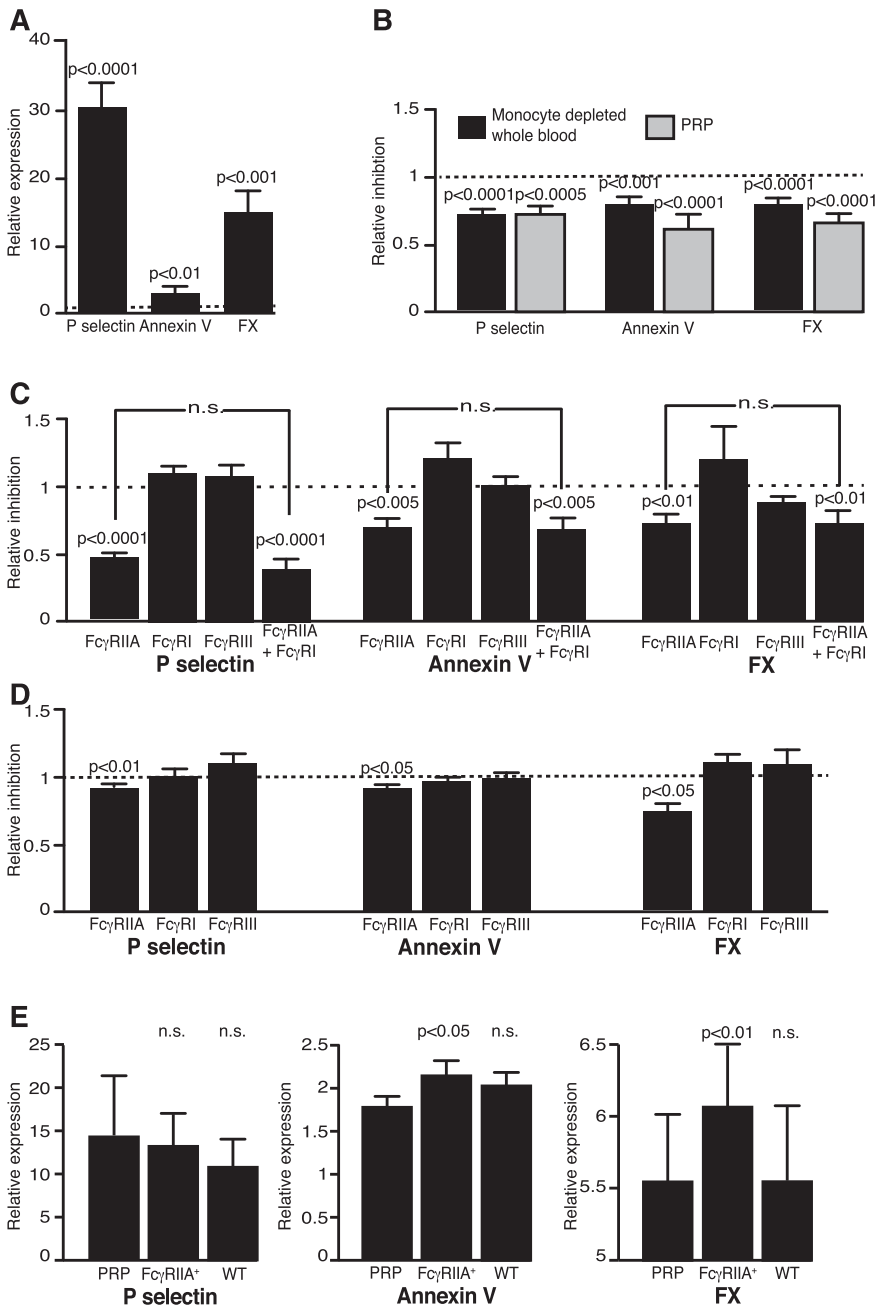
We hypothesized that in addition to direct platelet activation through FcγRIIA by HIT antibodies, monocytes provide the second signal through platelet PAR1 needed to support formation of coated platelets. Indeed, blocking PAR1 with the selective nonpeptide inhibitor SCH

79797 (Santa Cruz Biotechnology) significantly decreased binding of Annexin V to platelets stimulated by KKO plus PF4 in a dose-dependent manner, whereas the inhibition of P-selectin expression was significantly affected only at high concentrations of the inhibitor and never reached the magnitude of inhibition of Annexin V binding (Figure 7A). This indicates that direct activation of platelets in HIT through FcγRIIA makes an important contribution to P-selectin expression, whereas phosphatidylserine expression and formation of coated platelets requires a second signal through the PAR1 receptor. In the microfluidic model, blocking PAR1 receptors significantly decreased platelet accretion (Figure 7B) and had a dramatic effect on fibrin deposition (Figure 7C), further supporting the role of thrombin as a mediator of the highly prothrombotic state of HIT.

## Discussion

Thrombosis is far more prevalent in patients with HIT than in those with other antiplatelet antibody-mediated causes of thrombocytopenia.<sup>41</sup> One potential explanation for this difference may be that in HIT, monocytes, neutrophils, and endothelial cells are targeted for activation as well.<sup>11,36,42,43</sup> However, the involvement and mechanism by which these cells contribute to thrombosis has received far less attention than platelets. We have shown previously that PF4 binds to monocyte cell surface GAGs with greater avidity than to platelet GAGs and that binding of HIT antigenic complexes to monocytes is more resistant to dissociation by heparin.<sup>11</sup> We have also shown that depletion of monocytes using clodronate liposomes attenuates thrombus formation in a passive murine model of HIT, but the mechanism underlying this finding was difficult to delineate in the whole animal and the relevance of these findings to humans remained to be demonstrated.

In this study, we use a microfluidic system, human cells, and whole blood, to assess the role of monocytes in two salient features of antibody-induced thrombosis in HIT (ie, platelet adhesion/aggregation and fibrin formation on a VWF-coated surface). We used a VWF-coated surface because deposition of platelets on injured or inflamed endothelium largely depends on VWF released from activated endothelial cells. This experimental set-up does not perfectly replicate conditions seen in a patient treated with heparin, but our comparison with *in vivo* studies in mice show that it does provide a relevant

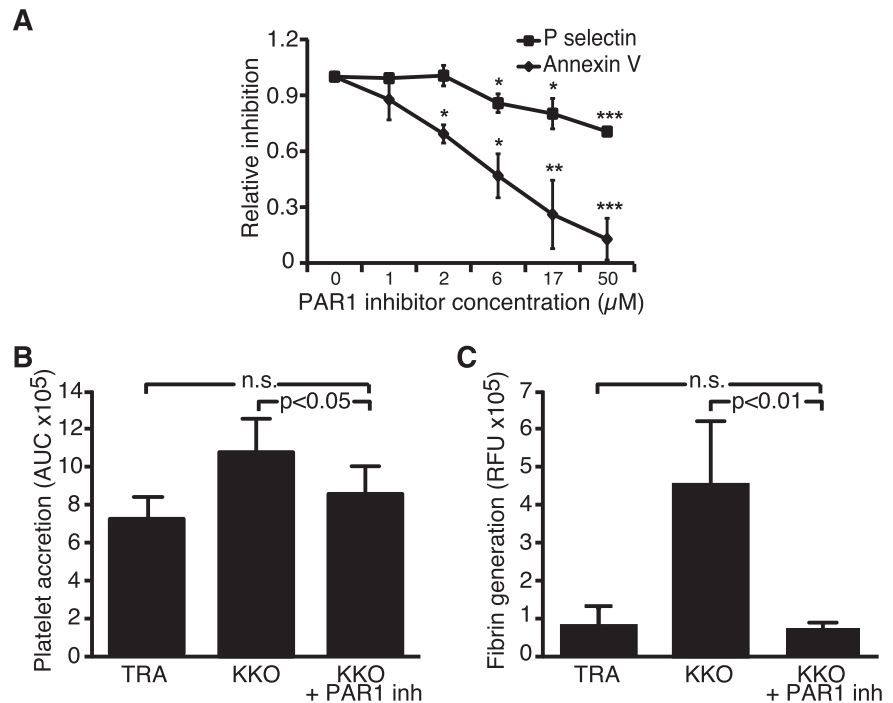


platform that provides insight into *in vivo* observations (supplemental Figure 2). Depletion of monocytes from whole blood attenuates platelet accretion and fibrin deposition, and monocyte repletion largely restores both outcomes. Further, monocytes, like platelets, are activated by HIT immune complexes through Fc $\gamma$ RIIA. Our findings differ from those implicating Fc $\gamma$ RI.<sup>31</sup> However, they do not exclude the possibility that Fc $\gamma$ RI receptors contribute at later time points, as we measured outcome at 30 minutes, which might reflect the de-encryption of TF, whereas the studies invoking Fc $\gamma$ RI measured *de novo* synthesis of TF at 6 hours.

Our results implicate activation of at least two cell types, platelets and monocytes, in HIT, and indicate that convergence of downstream activation pathways in these two cell types contributes to the procoagulant state. Binding of PF4/HIT antibody complexes to monocyte GAGs leads to activation of Fc $\gamma$ RIIA and downstream

signaling via a Syk-dependent pathway, inducing TF expression and thrombin generation. Monocytes might also be activated upon phagocytosis of immune complex coated platelets through Fc $\gamma$ RIIA, but the relative importance of these two mechanisms will require further study. Thrombin then cleaves platelet PAR1 and activates a GPCR-dependent pathway. Platelets are also activated directly through an Fc $\gamma$ RIIA ITAM pathway by HIT immune complexes bound to their surface. Direct activation through Fc $\gamma$ RIIA leads to robust P-selectin expression on platelets, whereas dual activation of platelets through a thrombin-mediated GPCR pathway and a Fc $\gamma$ RIIA ITAM pathway leads to the formation of procoagulant coated platelets,<sup>39</sup> which might help distinguish platelet involvement in HIT from other antibody-mediated thrombocytopenias characterized by bleeding. Additional studies are needed to identify the sequence or concurrence and interaction between these two pathways *in vivo* and whether

**Figure 7. Effect of PAR1 inhibition on P-selectin expression, Annexin V binding, platelets adhesion, and fibrin generation.** (A) Whole blood was pre-incubated with increasing concentrations of selective nonpeptide PAR1 receptor inhibitor SCH 79797 and then stimulated with PF4 and KKO. The data are expressed as inhibition of platelet stimulation when samples pre-incubated with the PAR1 inhibitor were compared with samples pre-incubated with vehicle.  $N = 3$ , each in duplicate. One sample  $t$  tests were used to determine the significance of inhibition when compared with 1, no inhibition. \* $P < .05$ ; \*\* $P < .01$ ; \*\*\* $P < .005$ . (B-C) Microfluidic studies were completed using human whole blood where platelet accretion (B) is represented as AUC over 15 minutes and fibrin deposition (C) as the sum of the relative fluorescent units. Samples were pre-incubated with 10  $\mu$ M SCH 79797 or vehicle, and then stimulated with PF4 and KKO or isotype control antibody TRA. Data are presented as mean  $\pm$  SEM.  $N = 9$  in both (B-C). All samples were run in parallel and paired  $t$  tests were employed on the raw data to assess significance.



quantification of coated platelets can be used to identify patients with HIT who are at high risk for thrombosis. These data are compatible with the benefits of direct thrombin inhibition drugs in the treatment of HIT. They also suggest that inactivation of additional inflammatory and proteolytic pathways in monocytes and other cell types in HIT may help to ameliorate the inability of direct thrombin inhibition drugs to fully protect against new thromboembolic events,<sup>44</sup> and suggest that targeting upstream cell-specific pathways might provide a more robust and disease-specific approach to intervention.

The relative contribution of a monocyte/macrophage-directed pathway vs direct platelet activation in HIT also requires further investigation. Monocytes, with their higher cell surface avidity for PF4 than platelets, may be a target for pathogenic HIT antibodies even before platelets are fully activated and while free PF4 is limited. This would lead to increased expression of TF and generation of thrombin, consistent with monocyte-driven thrombosis, followed by clearance of activated monocytes from the circulation. Once the level of PF4 from transactivated platelets reaches a threshold level, activated platelets may become the predominant target of HIT antibodies, providing a second signal leading to direct platelet activation and clearance. This proposed change in primary cell target from monocytes to platelets will need additional experimental and clinical study to validate, but if confirmed, may affect early diagnosis of risk and lead to novel forms of medical intervention.

In conclusion, our studies show that monocytes contribute to the prothrombotic nature of HIT. Targeting of monocytes by HIT antibodies may distinguish HIT from other immune thrombocytopenias. Fc $\gamma$ RIIA-mediated activation of the ITAM/Syk pathway in monocytes as well as platelets is involved. Monocyte activation leads to TF expression and generation of thrombin, which then promotes platelet activation via dual stimulation of both the GPCR and ITAM pathways, resulting in highly reactive, coated platelets as well as enhancing fibrin generation. We also propose that the monocyte/macrophage-directed prothrombotic state occurs early in HIT given the higher avidity of monocytes for PF4 compared with platelets. As HIT progresses and more PF4 is released (and perhaps as monocyte depletion occurs), the pathogenesis underlying HIT may evolve toward being more

platelet-specific. Testing this model, involving early-onset monocyte activation and thrombin generation in the initial stages of HIT, and more direct platelet activation as the disease progresses, requires confirmation in animal models and in affected patients. Understanding the pathway of monocyte transactivation of platelets may assist in the development of diagnostic tools to assess risk in HIT and more directed therapeutic interventions.

## Acknowledgments

The authors thank Dr Gowthami M. Arepally at Duke University for generously supplying KKO and RTO hybridoma cells, Dr Rodney Camire at the University of Pennsylvania and CHOP for supplying anti-FX antibody, and Dr Uma Sinha at Portola Pharmaceuticals for the Syk inhibitor, PRT318.

Support for this research was provided by the American Society of Hematology summer student awards (V.T.), grants from the National Institutes of Health, National Heart, Lung, and Blood Institute (P01 HL110860) (L.R., M.P., D.B.C., and S.E.M.) and (R01 HL115187-01A1) (X.L.Z.), and by the Program for Competitive Growth of Kazan Federal University (I.A.).

## Authorship

Contribution: V.T. was the primary investigator who carried out most of the microfluidic experiments and confocal microscopy studies, performed initial data analysis and interpretation, and wrote the first draft of the manuscript; D.M. performed Fc $\gamma$ R blocking studies; H.S.A. performed microfluidic studies with mouse blood; I.A. performed the mouse monocyte isolation studies; V.H. performed the cremaster laser injury model studies; X.L.Z. provided key materials to complete these studies; D.B.C. contributed to the design and interpretation of the described studies and helped with manuscript



revision; S.E.M. provided important insights and direction to the manuscript; M.P. provided overall direction, helped design the experiments, and contributed to manuscript preparation; and L.R. was the senior investigator who designed and supervised or carried out the described studies, and was responsible for the final data analysis and interpretation.

Conflict-of-interest disclosure: S.E.M. previously received research funding from Portola Pharmaceuticals. The remaining authors declare no competing financial interests.

Correspondence: Lubica Rauova, The Children's Hospital of Philadelphia, 3615 Civic Center Blvd, ARC Suite 316, Philadelphia, PA 19104; e-mail: lubica@e-mail.chop.edu.

## References

- Amiral J, Bridey F, Dreyfus M, et al. Platelet factor 4 complexed to heparin is the target for antibodies generated in heparin-induced thrombocytopenia. *Thromb Haemost*. 1992;68(1):95-96.
- Sachais BS, Litvinov RI, Yarovoi SV, et al. Dynamic antibody-binding properties in the pathogenesis of HIT. *Blood*. 2012;120(5):1137-1142.
- Warkentin TE, Kelton JG. A 14-year study of heparin-induced thrombocytopenia. *Am J Med*. 1996;101(5):502-507.
- Greinacher A, Farmer B, Kroll H, Kohlmann T, Warkentin TE, Eichler P. Clinical features of heparin-induced thrombocytopenia including risk factors for thrombosis. A retrospective analysis of 408 patients. *Thromb Haemost*. 2005;94(1):132-135.
- Warkentin TE, Sheppard JA, Heels-Ansdell D, et al; Canadian Critical Care Trials Group; Australian and New Zealand Intensive Care Society Clinical Trials Group. Heparin-induced thrombocytopenia in medical surgical critical illness. *Chest*. 2013;144(3):848-858.
- Greinacher A, Eichler P, Lubenow N, Kwasny H, Luz M. Heparin-induced thrombocytopenia with thromboembolic complications: meta-analysis of 2 prospective trials to assess the value of parenteral treatment with lepirudin and its therapeutic aPTT range. *Blood*. 2000;96(3):846-851.
- Chong BH, Castaldi PA, Berndt MC. Heparin-induced thrombocytopenia: effects of rabbit IgG, and its Fab and FC fragments on antibody-heparin-platelet interaction. *Thromb Res*. 1989;55(2):291-295.
- Kelton JG, Sheridan D, Santos A, et al. Heparin-induced thrombocytopenia: laboratory studies. *Blood*. 1988;72(3):925-930.
- Arepally G, Cines DB. Pathogenesis of heparin-induced thrombocytopenia and thrombosis. *Autoimmun Rev*. 2002;1(3):125-132.
- Rauova L, Zhai L, Kowalska MA, Arepally GM, Cines DB, Poncz M. Role of platelet surface PF4 antigenic complexes in heparin-induced thrombocytopenia pathogenesis: diagnostic and therapeutic implications. *Blood*. 2006;107(6):2346-2353.
- Rauova L, Hirsch JD, Greene TK, et al. Monocyte-bound PF4 in the pathogenesis of heparin-induced thrombocytopenia. *Blood*. 2010;116(23):5021-5031.
- Nader HB. Characterization of a heparan sulfate and a peculiar chondroitin 4-sulfate proteoglycan from platelets. Inhibition of the aggregation process by platelet chondroitin sulfate proteoglycan. *J Biol Chem*. 1991;266(16):10518-10523.
- Ward JV, Packham MA. Characterization of the sulfated glycosaminoglycan on the surface and in the storage granules of rabbit platelets. *Biochim Biophys Acta*. 1979;583(2):196-207.
- den Dekker E, Grefte S, Huijs T, et al. Monocyte cell surface glycosaminoglycans positively modulate IL-4-induced differentiation toward dendritic cells. *J Immunol*. 2008;180(6):3680-3688.
- Wegrowski Y, Milard AL, Kotlarz G, Toulmonde E, Maquart FX, Bernard J. Cell surface proteoglycan expression during maturation of human monocytes-derived dendritic cells and macrophages. *Clin Exp Immunol*. 2006;144(3):485-493.
- Newman PM, Swanson RL, Chong BH. Heparin-induced thrombocytopenia: IgG binding to PF4-heparin complexes in the fluid phase and cross-reactivity with low molecular weight heparin and heparinoid. *Thromb Haemost*. 1998;80(2):292-297.
- Skipwith CG, Cao W, Zheng XL. Factor VIII and platelets synergistically accelerate cleavage of von Willebrand factor by ADAMTS13 under fluid shear stress. *J Biol Chem*. 2010;285(37):28596-28603.
- Arepally GM, Kamei S, Park KS, et al. Characterization of a murine monoclonal antibody that mimics heparin-induced thrombocytopenia antibodies. *Blood*. 2000;95(5):1533-1540.
- Cuker A, Arepally G, Crowther MA, et al. The HIT Expert Probability (HEP) Score: a novel pre-test probability model for heparin-induced thrombocytopenia based on broad expert opinion. *J Thromb Haemost*. 2010;8(12):2642-2650.
- Arepally G, Reynolds C, Tomaski A, et al. Comparison of PF4/heparin ELISA assay with the 14C-serotonin release assay in the diagnosis of heparin-induced thrombocytopenia. *Am J Clin Pathol*. 1995;104(6):648-654.
- Kirchhofer D, Moran P, Bullens S, Peale F, Bunting S. A monoclonal antibody that inhibits mouse tissue factor function. *J Thromb Haemost*. 2005;3(5):1098-1099.
- Eslin DE, Zhang C, Samuels KJ, et al. Transgenic mice studies demonstrate a role for platelet factor 4 in thrombosis: dissociation between anticoagulant and antithrombotic effect of heparin. *Blood*. 2004;104(10):3173-3180.
- Reilly MP, Sinha U, André P, et al. PRT-060318, a novel Syk inhibitor, prevents heparin-induced thrombocytopenia and thrombosis in a transgenic mouse model. *Blood*. 2011;117(7):2241-2246.
- Dale GL. Coated-platelets: an emerging component of the procoagulant response. *J Thromb Haemost*. 2005;3(10):2185-2192.
- Conant CG, Nevill JT, Zhou Z, Dong JF, Schwartz MA, Ionescu-Zanetti C. Using well-plate microfluidic devices to conduct shear-based thrombosis assays. *J Lab Autom*. 2011;16(2):148-152.
- George JN, Onofre AR. Human platelet surface binding of endogenous secreted factor VIII-von Willebrand factor and platelet factor 4. *Blood*. 1982;59(1):194-197.
- Malek AM, Alper SL, Izumo S. Hemodynamic shear stress and its role in atherosclerosis. *JAMA*. 1999;282(21):2035-2042.
- Reilly MP, Taylor SM, Hartman NK, et al. Heparin-induced thrombocytopenia/thrombosis in a transgenic mouse model requires human platelet factor 4 and platelet activation through FcγRIIIA. *Blood*. 2001;98(8):2442-2447.
- Suh JS, Aster RH, Visentin GP. Antibodies from patients with heparin-induced thrombocytopenia/thrombosis recognize different epitopes on heparin: platelet factor 4. *Blood*. 1998;91(3):916-922.
- Reilly MP, McKenzie SE. Insights from mouse models of heparin-induced thrombocytopenia and thrombosis. *Curr Opin Hematol*. 2002;9(5):395-400.
- Kasthuri RS, Glover SL, Jonas W, et al. PF4/heparin-antibody complex induces monocyte tissue factor expression and release of tissue factor positive microparticles by activation of FcγRI. *Blood*. 2012;119(22):5285-5293.
- Daëron M. Fc receptor biology. *Annu Rev Immunol*. 1997;15:203-234.
- Dougherty GJ, Selvendran Y, Murdoch S, Palmer DG, Hogg N. The human mononuclear phagocyte high-affinity Fc receptor, FcRI, defined by a monoclonal antibody, 10.1. *Eur J Immunol*. 1987;17(10):1453-1459.
- Rosenfeld SI, Looney RJ, Leddy JP, Phipps DC, Abraham GN, Anderson CL. Human platelet Fc receptor for immunoglobulin G. Identification as a 40,000-molecular-weight membrane protein shared by monocytes. *J Clin Invest*. 1985;76(6):2317-2322.
- Tamm A, Schmidt RE. The binding epitopes of human CD16 (Fc gamma RIII) monoclonal antibodies. Implications for ligand binding. *J Immunol*. 1996;157(4):1576-1581.
- Arepally GM, Mayer IM. Antibodies from patients with heparin-induced thrombocytopenia stimulate monocyte cells to express tissue factor and secrete interleukin-8. *Blood*. 2001;98(4):1252-1254.
- Lyon ME, Fine JS, Henderson PJ, Lyon AW. D-phenylalanyl-L-prolyl-L-arginine chloromethyl ketone (PPACK): alternative anticoagulant to heparin salts for blood gas and electrolyte specimens. *Clin Chem*. 1995;41(7):1038-1041.
- Kahn ML, Nakanishi-Matsui M, Shapiro MJ, Ishihara H, Coughlin SR. Protease-activated receptors 1 and 4 mediate activation of human platelets by thrombin. *J Clin Invest*. 1999;103(6):879-887.
- Batar P, Dale GL. Simultaneous engagement of thrombin and Fc gamma RIIA receptors results in platelets expressing high levels of procoagulant proteins. *J Lab Clin Med*. 2001;138(6):393-402.
- Dale GL, Friese P, Batar P, et al. Stimulated platelets use serotonin to enhance their retention of procoagulant proteins on the cell surface. *Nature*. 2002;415(6868):175-179.
- Kim KJ, Baek IW, Yoon CH, Kim WU, Cho CS. Thrombotic risk in patients with immune thrombocytopenia and its association with antiphospholipid antibodies. *Br J Haematol*. 2013;161(5):706-714.
- Xiao Z, Visentin GP, Dayananda KM, Neelamegham S. Immune complexes formed following the binding of anti-platelet factor 4 (CXCL4) antibodies to CXCL4 stimulate human neutrophil activation and cell adhesion. *Blood*. 2008;112(4):1091-1100.
- Cines DB, Tomaski A, Tannenbaum S. Immune endothelial-cell injury in heparin-associated thrombocytopenia. *N Engl J Med*. 1987;316(10):581-589.
- Kelton JG, Hursting MJ, Hedde N, Lewis BE. Predictors of clinical outcome in patients with heparin-induced thrombocytopenia treated with direct thrombin inhibition. *Blood Coagul Fibrinolysis*. 2008;19(6):471-475.